GLAST LAT SUBSYSTEM TECHNICAL DOCUMENT	Document # **LAT-TD-00844-D1**	Date Effective Draft 07/18/02
	Prepared by(s) Alex Moiseev	Supersedes None
	Subsystem/Office Anticoincidence Detector Subsystem	
Document Title **ACD Gain Calibration Test with Cosmic Ray Muons**		

Gamma-ray Large Area Space Telescope (GLAST)

Large Area Telescope (LAT)

ACD Gain Calibration Test with Cosmic Ray Muons

DRAFT

CHANGE HISTORY LOG

Revision	Effective Date	Description of Changes

1. Purpose

This study reports on test methods for verifying the performance of the ACD after assembly.

2. Definitions and Acronyms

ACD	The LAT Anti-Coincidence Detector Subsystem
ADC	Analog-to-Digital Converter
AEM	ACD Electronics Module
ASIC	Application Specific Integrated Circuits
BEA	Base Electronics Assembly
CAL	The LAT Calorimeter Subsystem
DAQ	Data Acquisition
EGSE	Electrical Ground Support Equipment
EMC	Electromagnetic Compatibility
EMI	Electromagnetic Interference
ESD	Electrostatic Discharge
FM	Flight Module
FMEA	Failure Mode Effect Analysis
FREE	Front End Electronics
GAFE	GLAST ACD Front End – Analog ASIC
GARC	GLAST ACD Readout Controller – Digital ASIC
GEVS	General Environmental Verification Specification
GLAST	Gamma-ray Large Area Space Telescope
HVBS	High Voltage Bias Supply
ICD	Interface Control Document
IDT	Instrument Development Team
I&T	Integration and Test
IRD	Interface Requirements Document
JSC	Johnson Space Center
LAT	Large Area Telescope
MGSE	Mechanical Ground Support Equipment
MLI	Multi-Layer Insulation
MPLS	Multi-purpose Lift Sling
PCB	Printed Circuit Board

PDR	Preliminary Design Review
PMT	Photomultiplier Tube
PVM	Performance Verification Matrix
QA	Quality Assurance
SCL	Spacecraft Command Language
SEL	Single Event Latch-up
SEU	Single Event Upset
SLAC	Stanford Linear Accelorator Center
TACK	Trigger Acknowledge
TDA	Tile Detector Assembly
T&DF	Trigger and Data Flow Subsystem (LAT)
TBD	To Be Determined
TBR	To Be Resolved
TSA	Tile Shell Assembly
TSS	Thermal Synthesizer System
TKR	The LAT Tracker Subsystem
VME	Versa Module Eurocard
WBS	Work Breakdown Structure
WOA	Work Order Authorization

3. Applicable Documents

Documents relevant to the ACD Photomultiplier Quality Plan include the following.

1. LAT-SS-00016, LAT ACD Subsystem Requirements – Level III Specification
2. LAT-SS-00352, LAT ACD Electronics Requirements – Level IV Specification
3. LAT-SS-00437, LAT ACD Mechanical Requirements – Level IV Specification
4. LAT-MD-00039-01, LAT Performance Assurance Implementation Plan (PAIP)
5. LAT-MD-00099-002, LAT EEE Parts Program Control Plan
6. LAT-SS-00107-1, LAT Mechanical Parts Plan
7. LAT-MD-00078-01, LAT System Safety Program Plan (SSPP)
8. ACD-QA-8001, ACD Quality Plan
9. LAT-TD-00760-D1 Selection of ACD Photomultiplier Tube

10. LAT-DS-00739-1 Specifications for ACD Photomultiplier Tubes

11. LAT-TD-00438-D2 LAT ACD Light Collection/Optical Performance Tests

12. LAT-TD-00720-D1 ACD Phototube Helium Sensitivity

13. LAT-DS-00740-1 Temperature Characteristics of ACD Photomultiplier Tubes

14. Response to RFQ 5-09742, Hamamatsu Photomultiplier Tube Proposal

4. **Introduction.**

The idea of the test is to run the ACD with cosmic ray muons and obtain pulse-height histograms, corresponding to a MIP, for each tile. These histograms will determine the tile light yield averaged over the tile area with muons distributed uniformly. It was shown (LAT-TD-00438-D2, LAT ACD Light Collection/Optical Performance Tests) that the loss of 2-3 fibers will cause the shift of MIP pulse-height peak by 10-15% . In testing the flight ACD, the readout will be gated by a VETO signal from ANY tile. The task is to find which tile coincidence combination is best for analyzing each particular tile. It can be done by simulating the ACD with the cosmic ray muons flux. To prove this approach, both simulations and real measurements were performed with BFEM ACD.

5. **BFEM Muon test.**

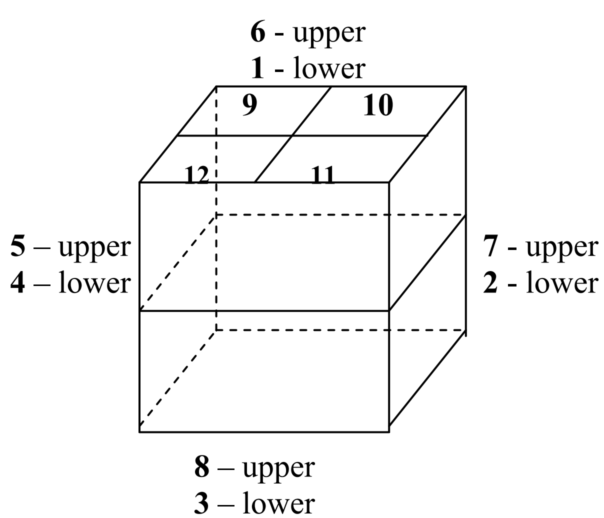

Fig.1 Tile Numbering for BFEM

The test was performed by pulse height analyzing the signals from each BFEM tile, gated by the signal from one of the tiles. It was repeated twice, first gating with tile 11 (one of the top tiles), and second gating with tile 8 (an upper side tile).

Simulations were done by GEANT 3.21/FLUKA with the exact BFEM geometry. The same tiles, 11 and 8, were used for event triggering. The muon flux used for the simulations was taken from A. Stephens (fig.2).

Comparison of simulation and test results. Table 1 shows the fraction of triggers showing signals in each tile. The pulse-height distributions obtained in the muon test and in the simulations, both triggered by tile 8, are shown in fig. 3 and fig.4, respectively. (Similar results triggered by tile 11 are not shown here.) Comparison between simulation and test results show that they are consistent, and that the simulations can be used to develop the muon test technique for the flight ACD configuration.

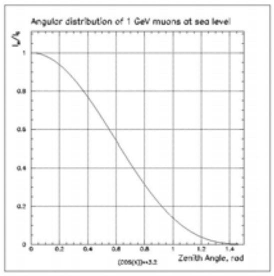

Fig.2 Muon flux angular dependence (Eμ>200 MeV)

Table 1. Fraction of triggers accompanied by a signal in each BFEM tile

Tile number	Test – gated by 11	Simulation – gated by 11	Test – gated by 8	Simulation – gated by 8
1	0.04	0.043	0.049	0.056
2	0.055	0.068	0.049	0.061
3	0.067	0.079		
4	0.049	0.042	0.052	0.062
5	0.065 ?	0.018	0.068	0.083
6	0.022	0.018	0.028	0.023
7	0.09	0.17	0.066	0.084
8	0.21	0.17		
9			0.018	0.019
10			0.017	0.018
11			0.11	0.18
12			0.11	0.17

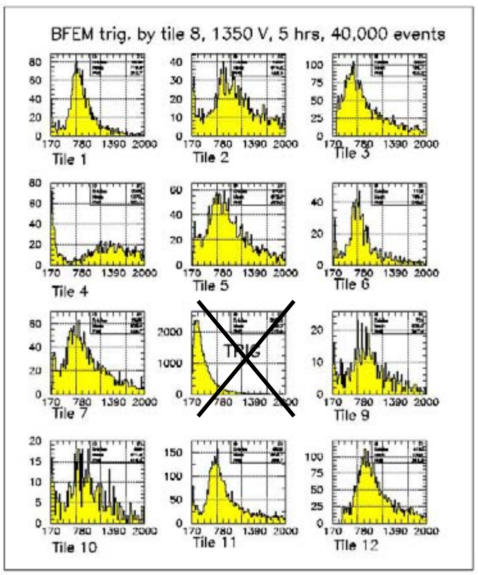

Fig.3 Muon test: Histograms from BFEM tiles triggered by tile 8

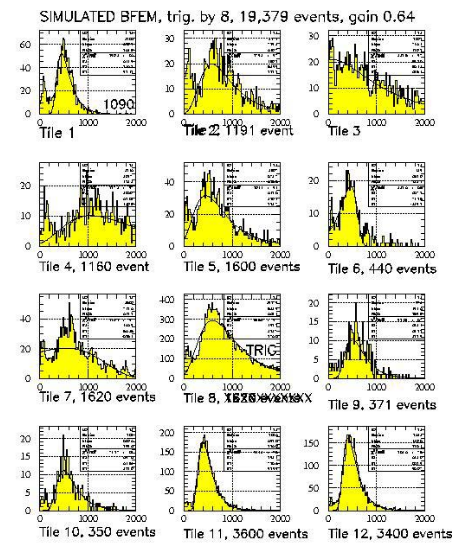

Fig.4 Simulations: Histograms from BFEM tiles triggered by tile 8

6. **Test of the Flight ACD** . The task is to find for each particular tile what other tiles can be used to trigger its analysis. The trajectories should be as normal to the tested tile surface as possible, with reasonable statistics to be collected from cosmic muons. The tile numbering used in the simulations is shown in Fig. 5. The simulation run corresponded to approximately 40 minutes of ACD running

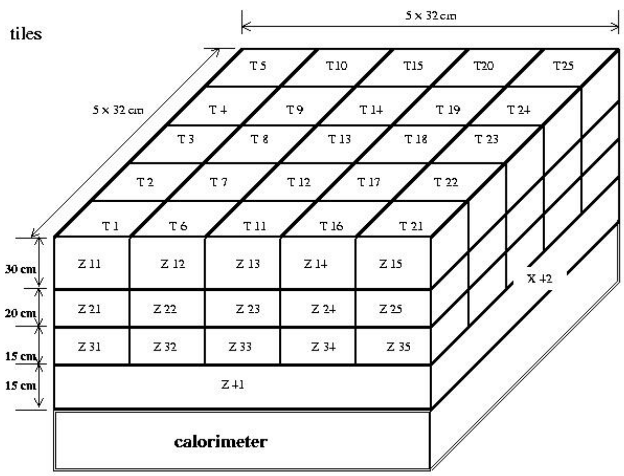

time, with 10-11 thousand triggers collected for each top tile. For each tile, the triggering tiles were carefully selected, and corresponding histograms are shown in figures below. For reliable fitting and MIP peak position determination, approximately 1,500 events are desirable in the histogram. Looking at the histograms, we see that the most difficult tiles to calibrate will be the upper side tiles (fig. 7), which will require 6-7 hours to obtain ~1,500 events. Limited calibration can be done within ~4 hours.

Fig.6 - Top tiles

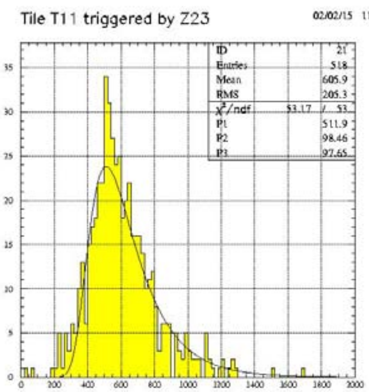

Tile T11 – middle of top edge

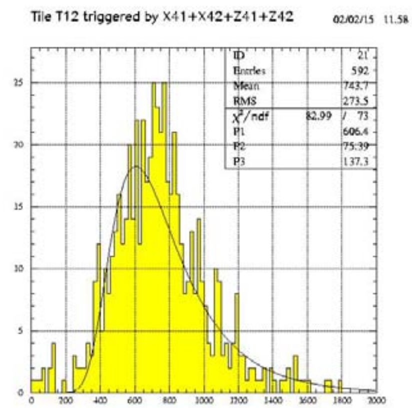

Tile T12 – next to the top central tile

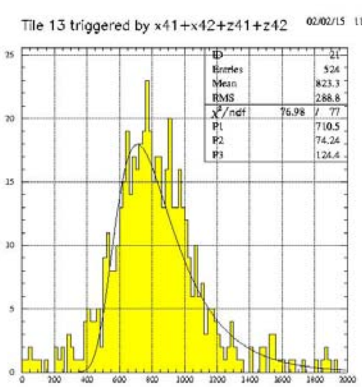

Tile T13 – top center tile

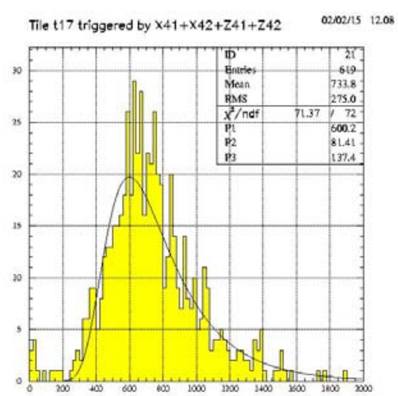

Tile T17 – diagonal from the top central tile

Fig. 7 - Side tiles

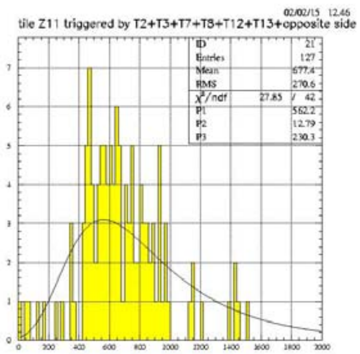

Tile Z11 – end tile in the side top row

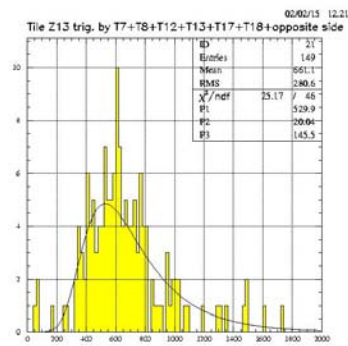

Tile Z13 – middle tile in the side top row

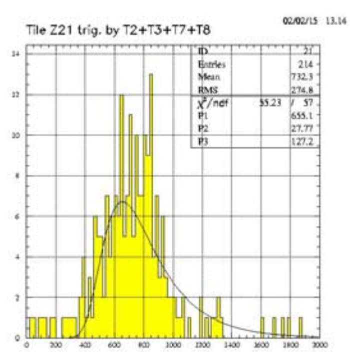

Tile Z21 – end tile in side second row

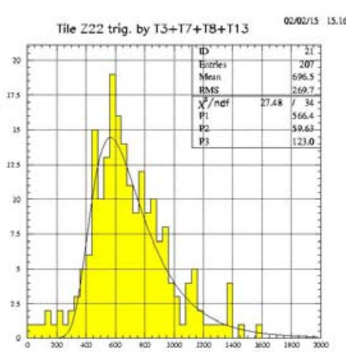

Tile Z22 – second tile from end in side second row

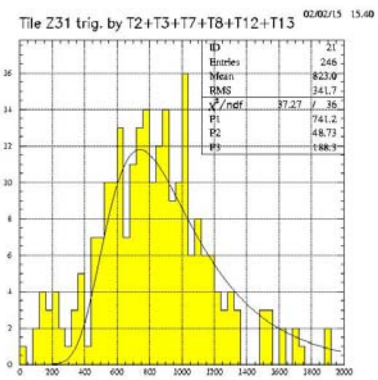

Tile 31 – end tile in side third row

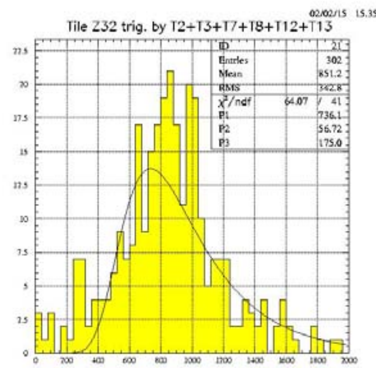

Tile Z32 – second tile from end in side third row

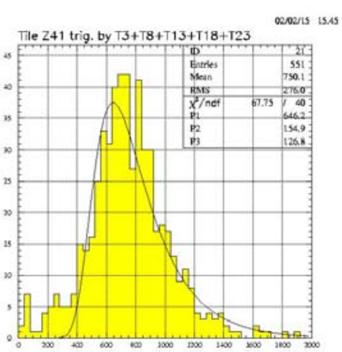

Tile Z41 - Long tile, side bottom row

Some remarks on the use of these histograms:

1. **Look at the quality of the histogram. For those that have too few of events, project how would it look at higher statistics.**
2. These histograms would be collected in ~40 min of running time, so one can estimate how much time will be needed to get a given number of events.

Note which tiles were used for selecting events in each histogram. Any suggestions to improve these choices would be welcome.

How many events do we need in the histogram for given peak position uncertainty?

I believe that the common mathematical approach to this estimate is complicated by the high variability of the particle paths in the tile and the desired reduction of the number of events needed. Simulations seem to be the appropriate way to do this analysis. I did the following: Using the sea level muon flux in the simulations, the simulated pulse height distribution was fitted by a Landau distribution to find the peak position. This was repeated for 10 sets of approximately 2,500, 1,000, and 500 events in the histogram and the mean value and standard deviation (σ) was determined for each of these sets of 10 runs. This was done for the tile on the top of ACD (for which most of muons hit the tile around normal incidence). The results are given in Table 2. The examples of the pulse height distribution for the top tile, with 996 events and 511 events in the histograms, are given in fig. 8 and fig.9 (column 3 and 4 in the table) respectively. The histogram for the side ("bad") tile (374 events) is shown in fig. 10 (column 5 in the table). It is seen that the precision of the peak position fitting is surprisingly high, even for such small statistics as ~500 events. For the "bad" tile (the side one), there is a large variation of incident muon angles, and consequently the muon paths in the tile. Note that we are looking for a change in the light yield of 5% and more.

Table 2 Simulations of the peak position determination precision

Fitted MIP peak position	Top tile, ~2,500 evts	Top tile, ~1,000 evts	Top tile, ~500 evts	Side tile, ~400 evts, gain=1	Side tile, ~400 evts, gain=0.95
	330.8	329.9	332.2	487.3	467.4
	333.0	326.8	338.2	495.2	467.2
	336.7	336.6	324.5	510.3	462.8
	340.9	338.4	331.5	481.3	489.9
	330.7	335.0	340.9	482.1	478.9
	334.9	330.9	348.4	491.9	539.5 ♣
	331.0	336.0	326.8	509.5	447.1
	336.8	339.1	343.0	510.9	482.1
	331.2	339.5	336.5	511.7	482.5
	336.2	334.8	350.8	521.1	476.4
Mean ±σ	334.2±3.4 (1%)	334.7±4.3 (1.3%)	337.3±8.7 (2.6%)	500.1±13.8 (2.8%)	478.7±24 (5%)

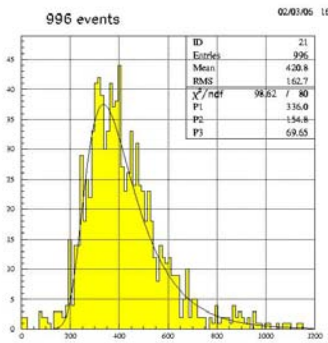

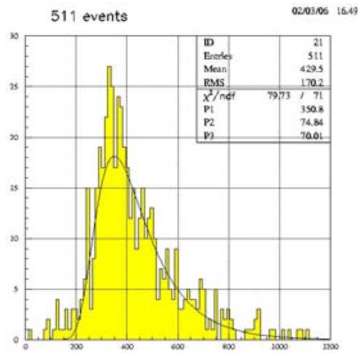

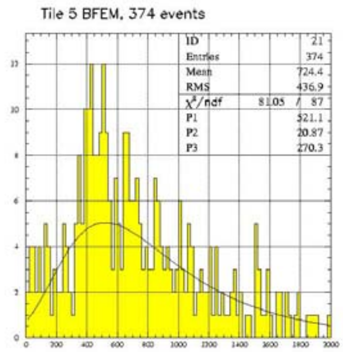

Fig. 8 Top tile, 996 events **Fig.9** Top tile, 511 events **Fig. 10** side tile, 374 events

7. **<u>The back-up option for testing the flight ACD</u>**. Another way to do the gain calibration test is to look at all tile histograms in a muon self-triggering mode, meaning that all signals recorded in given tile, will be used for the analysis. The advantage of this approach is that for ~1 hour of instrument running there will be from 3,000 to 15,000 events in the histograms (depending on the tile), which provides a very reliable and precise peak position determination. The disadvantage of this approach is that the histograms for some tiles, especially the side tiles, will be very dependent on the muon angular distribution. No external triggering will be used, so the angular range of particles causing the triggering will be 2π for every tile. The incident flux angular dependence could cause uncertainty if that angular distribution varies. The muon flux angular distribution is constant for a given location, so this particular approach can be successfully used for repeated functional tests performed in the same place. After moving to another place, re-calibration must be done using the approach described earlier, similar to fig. 6 and 7, with histograms selected by appropriate triggering. The histograms for the same tiles, in self-triggering mode, are presented in fig. 11 and 12, which illustrate the high statistics achieved with this approach.

Fig. 11 – Top tiles in self-triggering mode

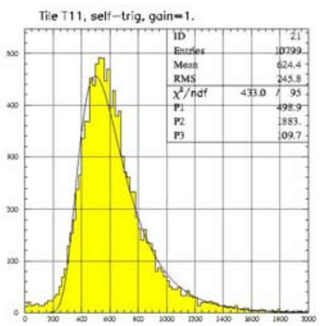

Tile T11 – middle tile in the edge row

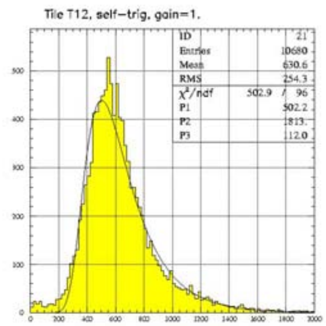

Tile T12 – next to the central tile

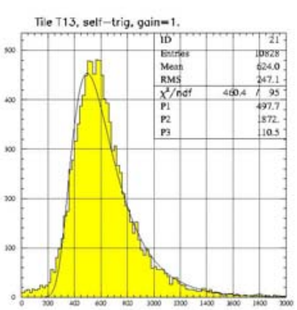

Tile T13 – top center tile

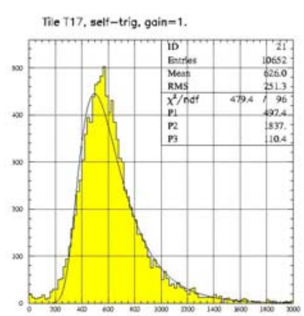

Tile T17 – diagonal from the central tile

Fig. 12 – Side tiles

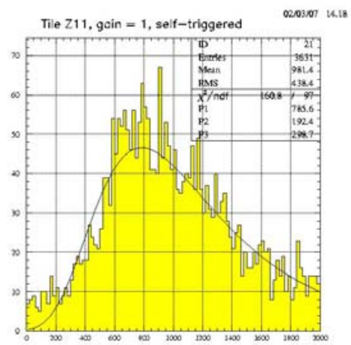

Tile Z11 – end tile in the top row

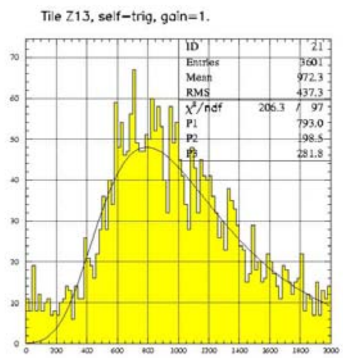

Tile Z13 – middle tile in the top row

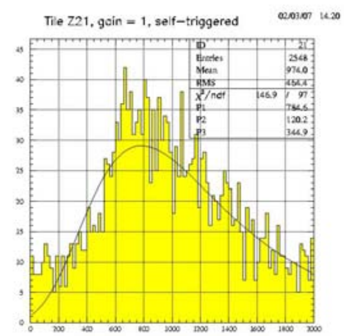

Tile Z21 – end tile in the second row

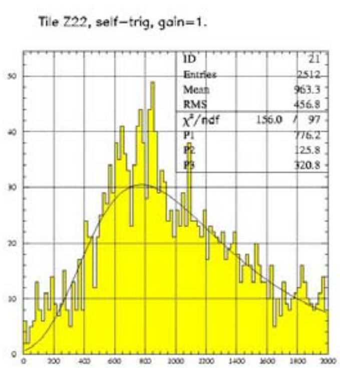

Tile Z22 – second tile from end in side second row

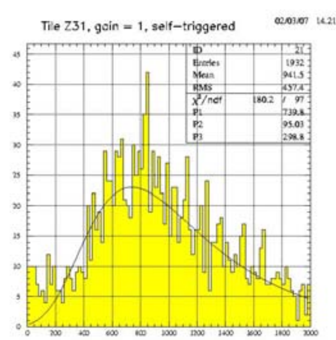

Tile Z31 – end tile in 3-rd row

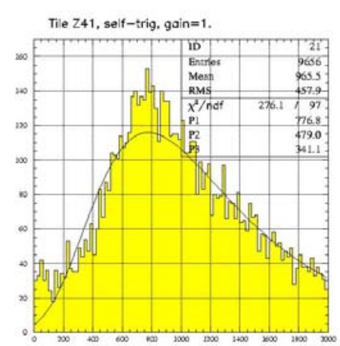

Tile Z41 – Long tile bottom row

How sensitive is the self-triggering mode to a gain change? A gain change of 5% was simulated. A similar situation was experimentally tested and proven with muons on BFEM. A simulation identical to that given above, but with a gain of 0.95 was performed. The MIP peak positions for these runs are given in the Table 3 along with the statistics in each corresponding histogram.

Tile	Statistics for 40 min	Peak position for gain = 1	Peak position for gain = 0.95	Ratio
T11	10,650	498.9	472.7	0.947
T12	10,680	502.2	476.4	0.949
T13	10,828	497.7	471.6	0.947
T17	10,651	497.4	471.6	0.948
Z11	3,631	785.6	748.9	0.953
Z13	3,601	793.0	756.7	0.954
Z21	2,547	784.6	748.8	0.954
Z22	2,512	776.2	729.7	0.940
Z31	1,930	739.8	711.2	0.961
Z32	1,944	765.5	735.8	0.961
Z41	9,658	776.8	738.0	0.950

The results obtained demonstrate that the sensitivity of this approach is quite adequate (5% gain change detectable).

8. **Conclusion**.

I believe that the gain calibration test should be done as follows:

1. During ACD I&T –
   a) gain calibration with muon hodoscope for each tile. This will be the most precise measurement (almost free from the uncertainty introduced by the different muon arrival direction). These results will serve as a reference in case of unclear future test results.
   b) a muon run for 8-10 hours, with triggering from any tile. The results will be treated in two ways – selecting triggers, and self-triggering. In both cases, the statistics reduction will be used to understand the stability of the results

2. In all other ACD test –Muon runs will be used for the available time, and depending on that time, the analysis approach will be selected. If visible performance change is noted, more careful testing must be performed, possibly requiring more time. In extreme cases, when tile replacement is contemplated, a muon hodoscope test should be performed before making the replacement decision.